and Applications, Institute of Energy Symp. Ser., No. 4, London (Nov., 1980).
Ross, I., J. F. Davidson Report at Int. Conf. Fluidized Combustion, Systems and Applications, Institute of Energy Symp. Ser., No. 4, London (Nov., 1980).
Vaux, W. G., "Attrition of Particles in the Bubbling Zone of a Fluidized Bed," Proceedings of the American Power Conference (1978).
Wells, J. W., R. P. Kirshnan, and C. E. Ball, "A Mathematical Model for Simulation of AFBC System," 6th Int. Conf. on Fluidized Bed Combustion, DOE, Atlanta, GA (April, 1980).
Zens, F. A., and N. A. Weil, "A Theoretical-Empirical Approach to the Mechanism of Particle Entrainment from Fluidized Beds," *AIChE J.*, No. 4, 4, 472 (1958).

Manuscript received June 19, 1981; revision received October 16, and accepted January 13, 1982

Feasible Specifications in Azeotropic Distillation

Feasible operating conditions are obtained for an azeotropic distillation tower using a nonlinear programming algorithm. The boil-up rate, fractional recovery of product, and bottoms purities of entrainer and by-product are adjusted to locate an overhead vapor stream that condenses into two liquid phases, but is in equilibrium with a single liquid phase on the top tray. A new objective function is introduced and minimized, subject to inequality constraints, using Powell's algorithm (1977). Results are obtained for dehydration of alcohol with benzene.

G. J. PROKOPAKIS and W. D. SEIDER

Department of Chemical Engineering
University of Pennsylvania
Philadelphia, PA 19104

SCOPE

In a classical paper, Benedict and Rubin (1945) define azeotropic distillation as "a process in which the substance added forms an azeotrope with one or more of the components and by virtue of this fact is present on most of the plates of the column in appreciable concentration." This definition correctly places emphasis on the need to select a mass separating agent that forms an azeotrope with one of the species to be separated, rather than the need to "break" an azeotrope.

Furthermore, a suitable entrainer, in the words of Benedict and Rubin, "forms non-ideal solutions with one or both of the components and thereby exaggerates the difference in volatility between them." Normally, entrainer is fed on the top tray, forming a low-boiling azeotrope with one or both of the species. Vapor with composition approaching the azeotrope is condensed and, for heterogeneous systems, the entrainer phase is decanted for reflux, as illustrated in Figure 1, for dehydration of alcohol.

In the typical configuration, one or more towers concentrate dilute alcohol to compositions approaching the alcohol-water azeotrope (shown schematically as a single processing step). In Figure 1a, nearly complete recovery of high purity alcohol is achieved in the azeotropic tower. The overhead vapor is condensed, a fraction is sent to a decanter, and the remainder is combined with the entrainer phase from the decanter and a small entrainer make-up stream as reflux to the azeotropic tower. The aqueous phase from the decanter is fed to the stripping tower, where nearly all of the water in the feed to the azeotropic tower is recovered in high purity. The overhead vapor, containing alcohol and water with some entrainer, is condensed and recycled to the decanter. Similar configurations have a common condenser with a portion of the condensate bypassing the decanter or a portion of the aqueous phase from the decanter recycled for reflux to the azeotropic tower. Such a decanter bypass stream or aqueous reflux is usually necessary to permit steady operation of the azeotropic tower with high recovery of alcohol in a high-purity bottoms product. Furthermore, for steady operation, these streams can be adjusted to respond to small changes in feed composition or product purity. The make-up stream replaces entrainer lost in parts-per-million concentration from the azeotropic and stripping towers.

In Figure 1b, the alcohol fed to the azeotropic tower is not entirely recovered. Instead alcohol and water in the bottoms of the stripping tower are recycled to the alcohol concentrators where water is recovered and alcohol is recirculated.

Azeotropic towers have been in operation for many years, but it is only recently that mathematical models have been sufficient to accurately trace the steep fronts in concentration and temperature. (See Figure 7, for example.) These fronts are extremely sensitive to small differences in the concentrations of entrainer and water in the nearly pure bottoms product and to the boil-up rate (Prokopakis and coworkers, 1981; Magnussen and coworkers, 1979). Furthermore, these variables must be carefully adjusted to prevent the models from predicting a vapor overhead stream that cannot be condensed to form two liquid phases, requiring that the overhead vapor stream from the stripping tower be condensable into two liquid phases, giving a high concentration of alcohol in the stripper bottoms, and low recovery of alcohol in the azeotropic tower.

In fact, it became so difficult to avoid operating conditions with low recovery of alcohol in the azeotropic tower, that we found it necessary to develop a strategy to avoid this problem. This has been accomplished by formulating a nonlinear programming problem with an appropriately selected objective function and inequality constraints.

0001-1541-83-6006-0049-$2.00.
G. J. Prokopakis is currently at Columbia University, New York, N.Y.

CONCLUSIONS

(1) The MESH (Material balance, Equilibrium, Summation of mole fractions, and Heat balance) equations for azeotropic distillation towers in the steady state require many iterations of the Ross and Seider algorithm (1981), which solves the equations for all trays simultaneously, probably because of the steep composition and temperature fronts. Our algorithm to solve the equations tray-by-tray (beginning with the reboiler, given specifications for the vapor boil-up rate, the recovery of alcohol in and the composition of the bottoms product) appears to be more efficient; however, an extensive comparison of computation times has not been undertaken.

(2) There is a narrow range of design variables, or specifications, that give high recovery of alcohol in the azeotropic tower and an overhead vapor that can be condensed into two liquid phases with positive flow rates in the decanter and decanter bypass streams.

(3) To obtain high recovery of alcohol in the azeotropic tower, the design variables should be adjusted to locate the liquid composition on the top tray, x_N, as close as possible to the ternary azeotrope, yet outside the binodal curve to avoid formation of a second liquid phase.

(4) There is a small window of overhead vapor concentration within which this objective is achieved. In this region, the overhead vapor condenses into two liquid phases, but is in equilibrium with a single liquid phase on the top tray. This region can easily be located with bubble point calculations.

(5) Conclusion 4 leads to the minimization problem P3, in which the design variables are adjusted to position the overhead vapor concentration within a feasible window, while satisfying the decanter equilibrium and material balance equations and the decanter bypass material balances with positive flow rates. P3 is solved efficiently and reliably using Powell's algorithm (1977).

(6) Given the solution to problem P3, the flow rate of the aqueous phase from the decanter is specified to permit routine clean-up by a stripping tower.

(7) Magnussen and coworkers (1979) report three steady states for the same specifications, but assume constant molal overflow and use the interaction coefficients for the UNIQUAC equation by Gmehling and Onken (1977). Unfortunately, to confirm these results, P3 could not be solved because the binodal curve computed with these coefficients is erroneous, giving benzene phases with less than 3% ethanol. Instead P3 was solved using the interaction coefficients of Prausnitz and coworkers (1980) and two of the three regimes presented by Magnussen and coworkers were confirmed. However, steady-state multiplicity was not confirmed.

PRIOR WORK

In this section, we review progress in the development of mathematical models for azeotropic towers before considering algorithms to solve the equations.

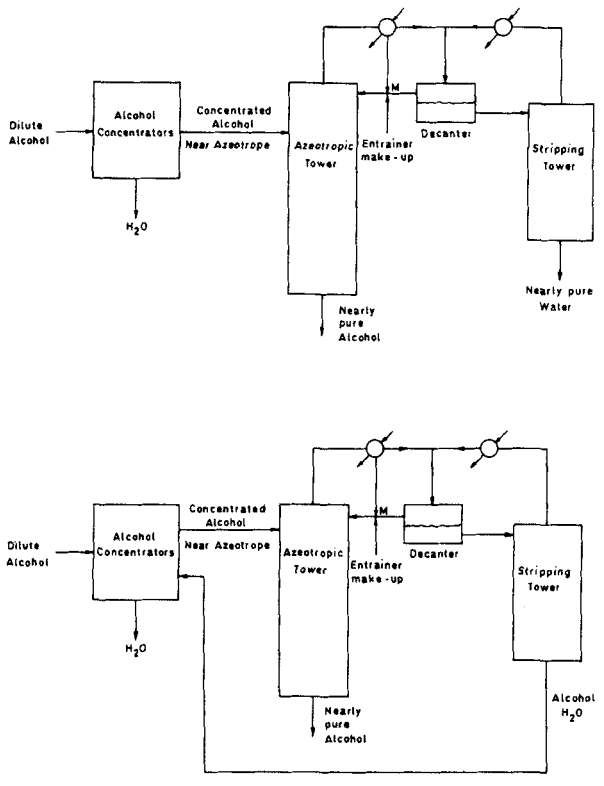

b

Figure 1. Configurations for dehydration of alcohol.

Mathematical Models

The earliest models were created to permit determination of the number of stages and location of the feed tray in azeotropic towers (Robinson and Gilliland, 1950) and involved material balances with graphs of relative volatility data. It was assumed that the vapor and liquid streams were in "constant molal overflow" in the steady state.

More recent models represent the interactions in nonideal solutions with equations that express the excess Gibbs free energy as a function of composition, temperature, and pressure; for example, the UNIQUAC, van Laar, Wilson, and NRTL equations (Prausnitz et al., 1980).

Van Dongen and Doherty (1979) and Magnussen and coworkers (1979) combined these solution models with the material balances. The former introduce a unique algorithm to determine the number of trays and the location of the feed tray, whereas the latter model an existing tower. Both assume operation with a constant molal overflow and in the steady state.

More complete models add the energy balance, eliminating the assumption of constant molal overflow. Black and coworkers (1972) created such a model to determine the number of stages and location of the feed tray, whereas Prokopakis and coworkers (1981) modelled an existing tower. They obtained flow rates that differ by 10–20%, especially in regions with steep concentration and temperature fronts.

The decanter can be adequately modelled with the material balances and a similar nonideal solution model. However, special care must be taken to utilize interaction coefficients that accurately represent the equilibrium data along the liquid-liquid binodal curve.

In recent work, Prausnitz and coworkers (1980) have developed a means of utilizing VLE data for the alcohol-water and alcohol-entrainer binary pairs and LLE data for the alcohol-entrainer-water system to give interaction coefficients for the UNIQUAC equation. They demonstrate fine agreement with the ternary LLE data. However, they do not include ternary VLE and VLLE data. This data would probably improve the fit near the heterogeneous ternary azeotrope (see Figure 2), an important region in the analysis of azeotropic towers.

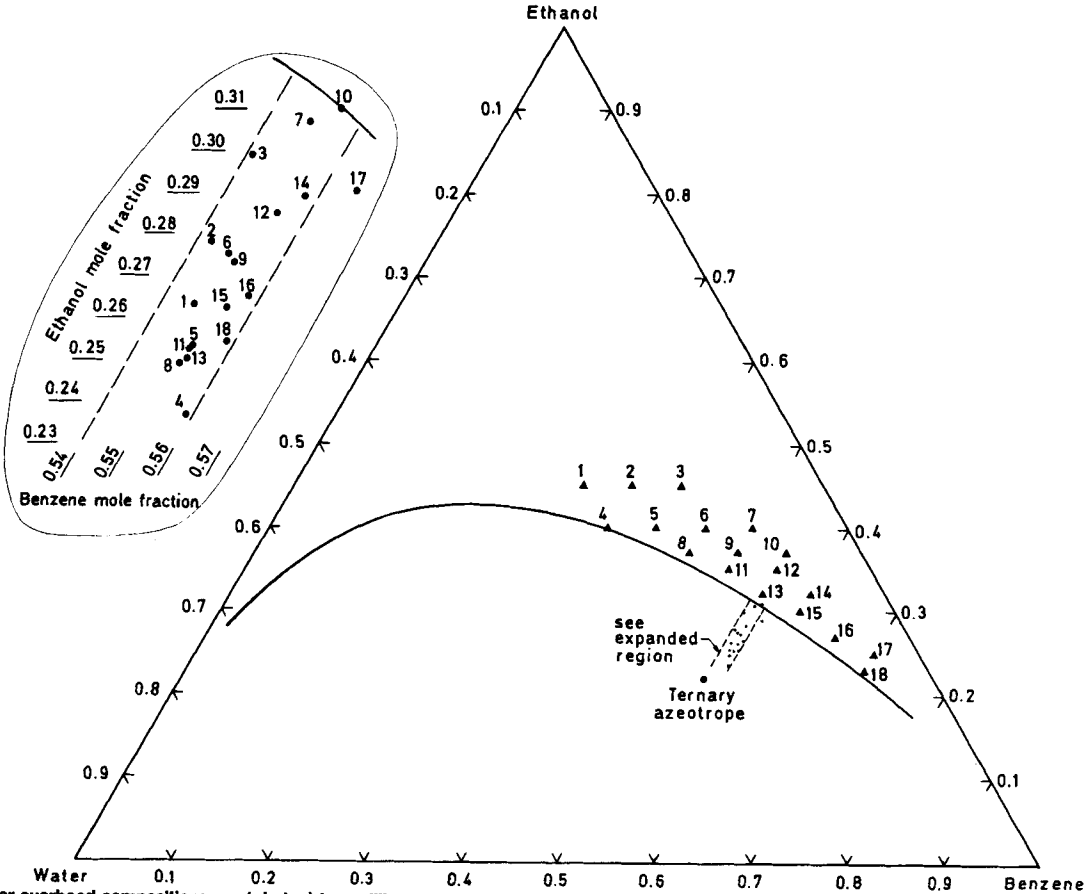

Figure 2. Vapor overhead compositions, $\underline{y}_N$ (circles) in equilibrium with liquid of composition, $\underline{x}_N$ (triangles). The UNIQUAC equation was used with the interaction coefficients of Prausnitz and coworkers (1980, p. 70). See Table 1.

Most designs do not involve two liquid phases on trays in the rectifying section. However, it is possible to operate most towers in this mode. To model such an azeotropic tower, it is necessary to include variables for the second liquid phase and to have interaction coefficients that accurately represent VLLE data (Prokopakis et al., 1981).

Models for dynamic simulation of azeotropic towers include terms to represent the rate of accumulation on the trays. Prokopakis and Seider (1980) prepared such a model assuming that the liquid hold-up varies with the liquid flow rate according to the Francis Weir Formula.

Algorithms

The steep concentration and temperature fronts, with the uncertainty of their location and their sensitivity to small changes in the bottoms composition and boil-up rate, make solution of the model equations more difficult. Consequently, specialized algorithms have evolved over the past 30 years.

To our knowledge, Robinson and Gilliland (1950) published the first algorithm for design of azeotropic towers. The algorithm requires specification of the bottoms flow rate and composition and solves the mass balances using relative volatility data, tray-by-tray, beginning with the reboiler and assuming constant molal overflow. The feed is saturated liquid and is introduced on the tray where its alcohol/water ratio matches that of the liquid phase. Trays are added to the rectifying section until the composition of the liquid entering the top tray lies within the binodal curve. Then, the composition of the organic reflux is approximated at the intersection of the straight line connecting the liquid compositions of streams leaving and entering the top tray ($\underline{x}_N$ and $\underline{x}_{N+1}$) and the binodal curve. The composition of the aqueous phase is given by its tie-line. These compositions for the decanter products are very approximate and lead to significant errors when combined with the material balances, ignoring the decanter bypass stream and assuming constant molal overflow, to compute the flow rates of all streams in the configuration.

Black and coworkers (1972) extended this algorithm using a more accurate model. In addition to the flow rate and mole fractions in the bottoms of the azeotropic tower, they specified the flow rate of the vapor boil-up. The MESH equations were solved, tray-by-tray beginning with the reboiler, to determine V_i, $\underline{y}_i$, L_{i+1}, $\underline{x}_{i+1}$ and T_{i+1}. In other respects, the algorithm is similar to that of Robinson and Gilliland. But, two important aspects of their work need further clarification:

(1) The mole fraction of water in the bottoms product is reduced by adding trays to the stripping section; presumably "to adjust conditions so that only a single liquid phase exists on all of the trays." However, the procedure for adjusting this mole fraction and its justification are not stated.

(2) Trays are added to the rectifying section until the alcohol mole fraction in the overhead vapor falls below a specified limit, indicating two liquid phases will form upon condensation. Then, the mole fraction of alcohol in the overhead vapor is varied slightly, but this strategy is not clearly stated.

Another problem with this algorithm involves the uncertainty in selecting a boil-up rate that leads to a good design. Excessive boil-up increases utility costs, while too little boil-up increases the number of trays.

Magnussen and coworkers (1979) used the Naphtali and Sandholm algorithm (1971) to solve the MES (material balance, equilibrium, and summation of mole fraction) equations for existing azeotropic towers. They assumed operation with constant molal overflow and, hence, omitted the energy balance. Whereas, Prokopakis and coworkers (1981) used the Ross and Seider algorithm (1981) to solve the MESH (MES and heat balance) equations, eliminating the assumption of constant molal overflow. These algorithms solve the MES or MESH equations for all of the trays simultaneously and were expected to be more efficient and reliable than tray-by-tray algorithms for simulation of existing towers. In

these studies, only the azeotropic tower was analyzed, it being assumed that the specifications gave a high recovery of alcohol in the azeotropic tower. Subsequently, we learned that the range of specified values to satisfy this requirement is very limited.

For high recovery of alcohol in the azeotropic tower it is necessary that: (a) the vapor composition leaving the top tray lie below the tie-line that connects the compositions of the organic and aqueous phases in the decanter (to permit the composition of the mixture of overhead vapor from the azeotropic and stripping towers to lie on the tie-line); and (b) the equilibrium equations and material balances for the decanter and the material balances for the decanter bypass stream be satisfied with positive flow rates. When condition a is not satisfied, to have two liquid phases in the decanter, the overhead vapor from the stripping tower must lie below the tie-line, and, consequently, the stripper bottoms product must be highly concentrated in alcohol with a low recovery in the azeotropic tower. The difficulty in satisfying these conditions is that small changes of entrainer and water (parts per million) in the nearly pure alcohol product and the boil-up rate can significantly displace the concentration and temperature fronts and change the overhead vapor composition.

For a three species system, the MESH equations for the azeotropic tower have four design variables, or specifications, in addition to the conditions of the feed and the tray pressures. Most computer programs permit specifications for a second feed, or reflux stream (i.e., L_{N+1}, $x_{N+1,alc}$, $x_{N+1,ent}$), and the bottoms flow rate, L_1, or the boil-up rate, V_1 (typical fourth specifications). However, many iterations are usually required to obtain a solution and, often, the desired purities in the bottoms product cannot be obtained or conditions a and b are not satisfied.

Alternatively, specification of the bottoms composition, $x_{1,ent}$ and $x_{1,wat}$, the recovery of alcohol in the bottoms product, R_{alc}, and the vapor boil-up rate, V_1, permits solution of the MESH equations for the reboiler and, subsequently, tray-by-tray up the tower, using the algorithm in the Appendix. Few iterations are required per tray and, for azeotropic distillation towers, this algorithm appears to be more efficient than solution of the MESH equations on all trays simultaneously. However, as previously, these specifications must be carefully selected to satisfy conditions *a* and *b*.

FEASIBLE OPERATING CONDITIONS

To satisfy conditions *a* and *b*, it helps to formulate an objective that can be achieved using an optimization procedure. One objective in azeotropic distillation is to locate the liquid composition on the top tray, $\underline{x}_N$, as close as possible to the ternary azeotrope, yet outside the binodal curve to avoid formation of a second liquid phase.

Consider the system, ethanol-water-benzene, with the binodal curve of Bancroft and Hubard (1942), at 298 K, in Figure 2. Prausnitz and coworkers (1980) computed interaction coefficients for the UNIQUAC equation using ternary LLE data and VLE data for the two miscible binary pairs (Table 1). Using these coefficients, the bubble point compositions, $\underline{y}$, were computed for a wide range of liquid compositions outside the binodal curve. As typical of systems with a ternary azeotrope, these vapor compositions lie in a narrow band surrounding the mole fraction of entrainer in the ternary azeotrope; 0.55 for benzene. Furthermore, most y_{alc} values lie above a lower limit, below which two liquid phases form (0.25 for this system), and below an upper limit defined by the binodal curve (0.31 for this system). Hence, it is possible to bound the region of overhead vapor mole fractions to achieve our objective; in this case, the bounds are $0.25 \leq y_{N,alc} \leq 0.31$ and $0.54 \leq y_{N,ent} \leq 0.56$. In this window, the overhead vapor condenses into two liquid phases, but is in equilibrium with a single liquid phase on the top tray.

Then, an alternate statement of the original objective is to locate $\underline{y}_N$ within the bounded region. This can be accomplished by solving the optimization problem:

TABLE 1. DATA FOR ETHANOL-BENZENE-WATER SYSTEM

UNIQUAC EQUATION

Prausnitz and Coworkers (1980)

	r	q	q'
Ethanol (1)	2.11	1.97	0.92
Benzene (2)	3.19	2.40	2.40
Water (3)	0.92	1.40	1.00

$a_{12} = -149.34$ $a_{21} = 1{,}131.13$
$a_{13} = -163.72$ $a_{31} = 573.61$
$a_{23} = 2057.42$ $a_{32} = 115.13$

Gmehling and Onken (1977)

	r	$q = q'$
Ethanol (1)	2.1055	1.972
Benzene (2)	3.1878	2.400
Water (3)	0.92	1.400

$a_{12} = -156.567$ $a_{21} = 850.609$
$a_{13} = 110.010$ $a_{31} = 200.054$
$a_{23} = 1072.790$ $a_{32} = 428.452$

Antoine Vapor Pressure (Gmehling and Onken, 1977)

$$ln\{P^s\} = a + \frac{b}{T + c}; \; P^s \text{ in bar, } T \text{ in K}$$

	a	b	c
Ethanol	12.05863	−3,667.705	−46.966
Benzene	9.22108	−2,755.642	−53.989
Water	11.96448	−3,984.923	−39.724

Enthalpy Parameters (Reid and Coworkers, 1977)

$$h = h_0 + c_1(T - T_0) + c_2(T^2 - T_0^2)/2 + c_3(T^3 - T_0^3)/3 + c_4(T^4 - T_0^4)/4$$

h in kJ/kgmol; $T_0 = 298$ K

Liquid	h_0	c_1	c_2	$c_3 \times 10^3$	$c_4 \times 10^6$
Ethanol	0	−67.4908	1.8438	−7.3027	10.5296
Benzene	0	−48.4300	5.0559	−14.2900	14.4190
Water	0	50.8300	0.2130	−0.6312	0.6486
Vapor	h_0	c_1	$c_2 \times 10^2$	$c_3 \times 10^4$	$c_4 \times 10^8$
Ethanol	43,713.9	1.0006	26.0838	−1.5935	3.9649
Benzene	33,645.0	36.8020	48.5700	−3.1860	7.9130
Water	44,529.3	33.9130	−0.3014	0.1520	−0.4857

$$\underset{V_1,R_{alc},x_{1,ent},x_{1,wat}}{\text{minimize}} \quad f = (y_{N,alc} - 0.25)^2 + (0.27 - y_{N,alc})^2 + (y_{N,ent} - 0.54)^2 + (0.56 - y_{N,ent})^2 \tag{1}$$

where the upper bound on $y_{N,alc}$ is reduced to assure that the window lies beneath the binodal curve defined by the experimental data of Norman (1945). The design variables (V_1, R_{alc}, $x_{1,ent}$, $x_{1,wat}$), are adjusted to minimize f subject to inequality constraints; for example:

$$\begin{gathered} 360 \le V_1 \\ 0.95 \le R_{alc} \le 0.9999 \\ 0 \le x_{1,ent} \le 10^{-4} \\ 0 \le x_{1,wat} \le 10^{-4} \\ 0.25 \le y_{N,alc} \le 0.27 \\ 0 \le r \le 1 \\ 0 \le L^e \end{gathered} \tag{2}$$

where V_1 is in mol/s. Note that two inequality constraints to bound $y_{N,alc}$ are redundant, but we have found that they significantly increase the rate of convergence when using Powell's algorithm, to be reviewed in the next section. The last two constraints are sufficient to satisfy feasibility condition *b*.

Alternatively, $y_{N,alc}$ and $y_{N,ent}$ could be specified (for example, 0.26 and 0.55, respectively) rather than R_{alc} and V_1. The remaining specifications would likely be $x_{1,ent}$ and $x_{1,wat}$, but these must be adjusted to position R_{alc} and V_1 in a feasible window that is limited and difficult to define. Furthermore, with specifications at the top and bottom of the tower, the MESH equations would probably be solved for all trays simultaneously, an algorithm that appears to be less efficient for azeotropic towers.

The formulation in Eqs. 1 and 2 can be generalized for azeotropic distillation towers with four or more chemical species. Bubble point calculations would be performed to determine a multidimensional band of vapor compositions in equilibrium with liquid compositions just outside of the region of two liquid phases. An additional design variable would be necessary for each species j, probably $x_{1,j}$, with bounds on these variables more difficult to set and the optimization problem more difficult to solve.

Powell's Nonlinear Programming Algorithm

Of the numerous algorithms for optimization of continuous objective functions with continuous first and second derivatives, subject to inequality constraints, Powell's algorithm (1977) is very well-suited because, it accounts for curvature in the nonlinear inequality constraints (six of the seven constraints in our final formulation are nonlinear; see P3) and moves rapidly into the feasible region with a well-designed unidirectional search procedure. The algorithm has been applied in several studies to optimize process flowsheets (Berna et al., 1980; Biegler and Hughes, 1981; Jirapongphan et al., 1980) and is particularly well-described by Jirapongphan (1980). Here, it will suffice to review the important features.

Consider the optimization problem:

$$\begin{aligned} &\text{minimize } f\{\underline{x}\} \\ &\text{subject to: } \underline{g}\{\underline{x}\} = 0 \\ &\qquad\qquad \underline{h}\{\underline{x}\} \ge 0 \end{aligned} \tag{P1}$$

where f is the objective function, $\underline{g}$ is a vector of equality constraints and $\underline{h}$ is a vector of inequality constraints. To solve problem P1, the Lagrangian is defined:

$$L\{\underline{x},\underline{\pi},\underline{\lambda}\} = f\{\underline{x}\} + \underline{\pi}^T\,\underline{g}\{\underline{x}\} + \underline{\lambda}^T(\underline{h}\{\underline{x}\} + \underline{z}^2) \tag{3}$$

where $\underline{\pi}$ is the vector of Lagrange multipliers, $\underline{\lambda}$ is the vector of Kuhn-Tucker multipliers, and $\underline{z}^2$ is the vector of slack variables ($\underline{h}\{\underline{x}\} = -\underline{z}^2$).

If $\underline{x}^*$ is a solution of P1, it is necessary that the Kuhn-Tucker conditions:

$$\left.\frac{\partial L}{\partial \underline{x}}\right|_{\underline{x}^*} = \nabla f\{\underline{x}^*\} + \left.\frac{\partial g}{\partial \underline{x}}\right|_{\underline{x}^*}^T \underline{\pi}^* + \left.\frac{\partial h}{\partial \underline{x}}\right|_{\underline{x}^*}^T \underline{\lambda}^* = 0$$

$$\underline{g}\{\underline{x}^*\} = 0$$

$$h_i\{\underline{x}^*\}\,\lambda_i^* = 0 \qquad i = 1, \ldots, m$$

$$\underline{h}\{\underline{x}^*\} \ge 0$$

$$\underline{\lambda}^* \ge 0$$

be satisfied at $\underline{x}^*$. Jirapongphan (1980) clearly presents Wilson's earlier observation that an iteration of the Newton-Raphson method for solution of the Kuhn-Tucker equations is equivalent to solving the quadratic programming problem:

$$\begin{aligned} &\underset{\underline{d}}{\text{minimize}}\ \nabla f\{\underline{x}^{(k)}\}^T\underline{d} + \tfrac{1}{2}\,\underline{d}^T\,\underline{\underline{\nabla^2 L}}\{\underline{x}^{(k)}\}\underline{d} \\ &\text{subject to: } \underline{\underline{J}}\underline{d} + \underline{g} = 0 \\ &\qquad\qquad \underline{\underline{K}}\underline{d} + \underline{h} \ge 0 \end{aligned} \tag{P2}$$

where $\underline{\underline{J}}$ is the Jacobian matrix of the equality constraints, $\underline{\underline{K}}$ is the Jacobian matrix of the inequality constraints, $\underline{d} = \underline{x}^{(k+1)} - \underline{x}^{(k)}$, and

$$\lim_{k\to\infty} \underline{x}^{(k)} = \underline{x}^*$$

Powell (1977) solves P2 during each iteration. Curvature of the constraints is accounted for in $\underline{\underline{\nabla^2 L}}$ which is approximated using the quasi-Newton update of Broyden, Fletcher, Goldfarb, and Shanno during each iteration. The BFGS update assures that the approximation to $\underline{\underline{\nabla^2 L}}$ is always positive definite, guaranteeing the existence of a solution to P2. Hence, convergence is obtained even when $\underline{\underline{\nabla^2 L}}$ is not positive definite.

The unidirectional search was developed by Han to move the design variables into the feasible region. Given $\underline{d}$, $\underline{\pi}^{(k+1)}$, and $\underline{\lambda}^{(k+1)}$, all computed by solution of P2, the parameter $\alpha^{(k+1)}$ is adjusted between 0 and 1 to minimize

$$\phi\{\underline{x}^{(k+1)}\} = f\{\underline{x}^{(k+1)}\} + \underline{\pi}^{*(k+1)^T}|\,\underline{g}\{\underline{x}^{(k+1)}\}| + \underline{\lambda}^{*(k+1)^T}|\min\{0,\underline{h}\{\underline{x}^{(k+1)}\}| \tag{4}$$

where

$$\underline{x}^{(k+1)} = \underline{x}^{(k)} + \alpha^{(k+1)}\underline{d} \tag{5}$$

$$\pi_i^{*(k+1)} = \max\{\pi_i^{(k+1)},\ \tfrac{1}{2}(\pi_i^{*(k)} + |\,\pi_i^{(k+1)}|)\} \tag{6}$$

1. Set k = 0 and guess $\underline{x}^{(0)}$
2. Compute $\underline{g}\{\underline{x}^{(k)}\}$, $\underline{h}\{\underline{x}^{(k)}\}$, $\nabla f\{\underline{x}^{(k)}\}$, $\underline{\underline{J}}\{\underline{x}^{(k)}\}$, $\underline{\underline{K}}\{\underline{x}^{(k)}\}$
3. Update $\underline{\underline{C}} \cong \underline{\underline{\nabla^2 L}}\{\underline{x}^{(k)}\}$
   For k = 0, set $\underline{\underline{C}}^{(k)} = \underline{\underline{I}}$
   For k > 0, update $\underline{\underline{C}}^{(k)}$ using the Broyden, Fletcher, Goldfarb, Shanno formula
4. Solve quadratic programming problem, P2, for
   $\underline{\pi}^{(k+1)}$, $\underline{\lambda}^{(k+1)}$, and $\underline{d}$
5. Let
   $$\underline{x}^{(k+1)} = \underline{x}^{(k)} + \alpha^{(k+1)}\,\underline{d}$$
   and perform the Han unidirectional search to find $\alpha^{(k+1)}$ $(0 \le \alpha \le 1)$
   $$\underset{\alpha^{(k+1)}}{\text{minimize}}\ \phi\{(\underline{x}^{(k+1)}\} = f\{\underline{x}^{(k+1)}\} + \underline{\pi}^{*(k+1)^T}|\,\underline{g}\{\underline{x}^{(k+1)}\}| + \underline{\lambda}^{*(k+1)^T}|\min\{0,\underline{h}\{\underline{x}^{(k+1)}\}|$$
   where
   $$\pi_i^{*(k+1)} = \max\{\pi_i^{(k+1)},\ \tfrac{1}{2}(\pi_i^{*(k)} + |\,\pi_i^{(k+1)}|)\}$$
   $$\lambda_i^{*(k+1)} = \max\{\lambda_i^{(k+1)},\ \tfrac{1}{2}(\lambda_i^{*(k)} + |\,\lambda_i^{(k+1)}|)\}$$
6. Convergence criteria satisfied?
   No. $k \leftarrow k + 1$

Figure 3. Powell's algorithm.

$$\lambda_i^{*(k+1)} = \max\{\lambda_i^{(k+1)},\ \tfrac{1}{2}(\lambda_i^{*(k)} + |\lambda_i^{(k+1)}|)\} \qquad (7)$$

Note that Eqs. 6 and 7 prevent the penalty terms in Eq. 4 from decreasing prematurely. This is particularly important near the boundary of an inequality constraint. When the $\lambda_i^{(k+1)}$ becomes zero because the constraint is satisfied, $\lambda_i^{*(k+1)}$ is decreased by averaging with the previous value. Note that once λ_i becomes non-zero it remains non-zero throughout the remaining iterations of Powell's algorithm.

In summary, the algorithm is presented in Figure 3.

Application of Powell's Algorithm for Azeotropic Distillation

To have the design variables near unity, we introduce the scaled variables

$$X_{1,ent} = x_{1,ent}/x_{1,ent}^U$$
$$X_{1,wat} = x_{1,wat}/x_{1,wat}^U \qquad (8)$$
$$\mathcal{V}_1 = V_1/V_1^L$$

where $x_{1,ent}^U$ and $x_{1,wat}^U$ are upper bounds in the inequality constraints ($=10^{-4}$ in Eqs. 2) and V_1^L is an estimate for the lower bound in V_1.

With these variables the optimization problem can be restated as:

$$\underset{\mathcal{V}_1, R_{alc}, X_{1,ent}, X_{1,wat}}{\text{minimize}} \quad f = (y_{N,alc} - y_{N,alc}^L)^2 + (y_{N,alc}^U - y_{N,alc})^2 + (y_{N,ent} - y_{N,ent}^L)^2 + (y_{N,ent}^U - y_{N,ent})^2$$

subject to:

$$h = \mathcal{V}_1 - 1 \geq 0 \qquad \text{(P3)}$$
$$h_2 = (R_{alc} - R_{alc}^L)(R_{alc}^U - R_{alc}) \geq 0$$
$$h_3 = X_{1,ent}(1 - X_{1,ent}) \geq 0$$
$$h_4 = X_{1,wat}(1 - X_{1,wat}) \geq 0$$
$$h_5 = (y_{N,alc} - y_{N,alc}^L)(y_{N,alc}^U - y_{N,alc}) \geq 0$$
$$h_6 = r(1 - r) \geq 0$$
$$h_7 = L^e \geq 0$$

Note that $h_2 - h_7$ are nonlinear functions of the design variables.

For each set of design variable values we solve the MESH equations, tray-by-tray, beginning at the bottom of the tower (see the Appendix for details). Alternatively, we could solve the MESH equations for all of the trays simultaneously, but for azeotropic distillation towers many iterations are usually necessary and the tray-by-tray algorithm is probably more efficient.

To evaluate r and L^e, the equations for the decanter must be solved. When the overhead vapor composition lies within the binodal curve, this is accomplished using the algorithm presented in the next section; otherwise, constraints h_6 and h_7 are set active, with $r = 1$ and $L^e = 0$.

For this problem, $\nabla f\{\underline{x}^{(k)}\}$ is evaluated by numerical perturbation (in Step 2 of Powell's algorithm) and the derivatives in $\underline{\underline{K}}$ are evaluated analytically for constraints $h_1 - h_4$ as shown in Figure 4. Derivatives for constraints $h_5 - h_7$ are evaluated by numerical perturbation.

Note that Boston (1978) has devised an algorithm that performs one iteration in the solution of the MESH equations for all trays simultaneously during each iteration of Powell's algorithm. We are experimenting with this approach, which promises to be more efficient, using the Ross and Seider (1981) algorithm for solution of the MESH equations. Our preliminary results indicate that it is difficult to satisfy conditions a and b with such a coupled algorithm.

The Decanter

To evaluate constraints h_6 and h_7, it remains to solve the equilibrium equations and material balances for the decanter and the material balances for the decanter bypass stream. We illustrate the solution of these equations for the configuration in Figure 1a.

$$\begin{array}{c} \\ h_1 \\ h_2 \\ h_3 \\ h_4 \\ h_5 \\ h_6 \\ h_7 \end{array}
\begin{bmatrix}
\mathcal{V}_1 & R_{alc} & X_{1,ent} & X_{1,wat} \\
1 & 0 & 0 & 0 \\
0 & R_{alc}^L + R_{alc}^U - 2R_{alc} & 0 & 0 \\
0 & 0 & 1 - 2X_{1,ent} & 0 \\
0 & 0 & 0 & 1 - 2X_{1,wat} \\
\dfrac{\partial h_5}{\partial \mathcal{V}_1} & \dfrac{\partial h_5}{\partial R_{alc}} & \dfrac{\partial h_5}{\partial X_{1,ent}} & \dfrac{\partial h_5}{\partial X_{1,wat}} \\
\dfrac{\partial h_6}{\partial \mathcal{V}_1} & \dfrac{\partial h_6}{\partial R_{alc}} & \dfrac{\partial h_6}{\partial X_{1,ent}} & \dfrac{\partial h_6}{\partial X_{1,wat}} \\
\dfrac{\partial h_7}{\partial \mathcal{V}_1} & \dfrac{\partial h_7}{\partial R_{alc}} & \dfrac{\partial h_7}{\partial X_{1,ent}} & \dfrac{\partial h_7}{\partial X_{1,wat}}
\end{bmatrix}$$

Figure 4. Jacobian matrix, $\underline{\underline{K}}$, for inequality constraints.

We begin with the material balances at point M:

$$V_N y_{N,alc} r + x_{alc}^e L^e - L_{N+1} x_{N+1,alc} = 0 \qquad (9)$$
$$V_N y_{N,ent} r + x_{ent}^e L^e - L_{N+1} x_{N+1,ent} + F_m = 0 \qquad (10)$$
$$V_N y_{N,wat} r + x_{wat}^e L^e - L_{N+1} x_{N+1,wat} = 0 \qquad (11)$$

where L^e is the flow rate of the entrainer phase from the decanter and $\underline{x}^e$ is its vector of mole fractions. $V_N, \underline{y}_N, L_{N+1}$, and $\underline{x}_{N+1}$ have been determined by solution of the MESH equations for the azeotropic tower and a small flow rate, F_m, is specified for the entrainer make-up stream.

The liquid-liquid equilibrium in the decanter is described by:

$$\gamma_{alc}\{\underline{x}^e, T^d\} x_{alc}^e = \gamma_{alc}\{\underline{x}^a, T^d\} x_{alc}^a \qquad (12)$$
$$\gamma_{ent}\{\underline{x}^e, T^d\} x_{ent}^e = \gamma_{ent}\{\underline{x}^a, T^d\} x_{ent}^a \qquad (13)$$
$$\gamma_{wat}\{\underline{x}^e, T^d\} x_{wat}^e = \gamma_{wat}\{\underline{x}^a, T^d\} x_{wat}^a \qquad (14)$$
$$x_{alc}^e + x_{ent}^e + x_{wat}^e = 1 \qquad (15)$$
$$x_{alc}^a + x_{ent}^a + x_{wat}^a = 1 \qquad (16)$$

where $\underline{\gamma}$ is the vector of activity coefficients evaluated at the composition of each phase and temperature of the decanter.

Equations 9–16 are solved for the eight unknowns, r, L^e, $\underline{x}^e$, and $\underline{x}^a$. However, good guesses for $\underline{x}^e$ and $\underline{x}^a$ are necessary to avoid the trivial solution; $\underline{x}^e = \underline{x}^a$. This is accomplished by guessing $\underline{x}^d$, the vector of mole fractions entering the decanter (initially assumed to be $\underline{y}_N$), within the binodal curve and solving Eqs. 12–16 with the material balances for the decanter to determine guesses for $\underline{x}^e$ and $\underline{x}^a$. With the guesses for $\underline{x}^e$, we have three Eqs. 9–11 in two unknowns (r,L^e). Hence, for a unique solution to exist:

$$\begin{vmatrix} V_N y_{N,alc} & x_{alc}^e & -L_{N+1} x_{N+1,alc} \\ V_N y_{N,ent} & x_{ent}^e & -L_{N+1} x_{N+1,ent} + F_m \\ V_N y_{N,wat} & x_{wat}^e & -L_{N+1} x_{N+1,wat} \end{vmatrix} = 0 \qquad (17)$$

and

$$x_{alc}^e [V_N y_{N,ent} L_{N+1} x_{N+1,wat} - V_N y_{N,wat}(L_{N+1} x_{N+1,ent} - F_m)] + x_{ent}^e [V_N y_{N,wat} L_{N+1} x_{N+1,alc} - V_N y_{N,alc} L_{N+1} x_{N+1,wat}] + x_{wat}^e [V_N y_{N,alc}(L_{N+1} x_{N+1,ent} - F_m) - V_N y_{N,ent} L_{N+1} x_{N+1,alc}] = 0 \qquad (18)$$

That is, to satisfy Eqs. 9–11, $\underline{x}^e$ must satisfy Eq. 18, which can be rewritten as

$$\hat{f} = \beta_1 x_{alc}^e + \beta_2 x_{ent}^e + \beta_3 x_{wat}^e = 0 \qquad (19)$$

This is accomplished by adjusting $\underline{x}^d$ to solve the optimization problem:

$$\underset{\underline{x}^d}{\text{minimize}} \quad f = \hat{f}^2$$

subject to:

$$\hat{h}_1 = (x_{alc}^d - 0.21)(0.29 - x_{alc}^d) \geq 0$$
$$\hat{h}_2 = (x_{ent}^d - 0.3)(0.6 - x_{ent}^d) \geq 0 \qquad \text{(P4)}$$

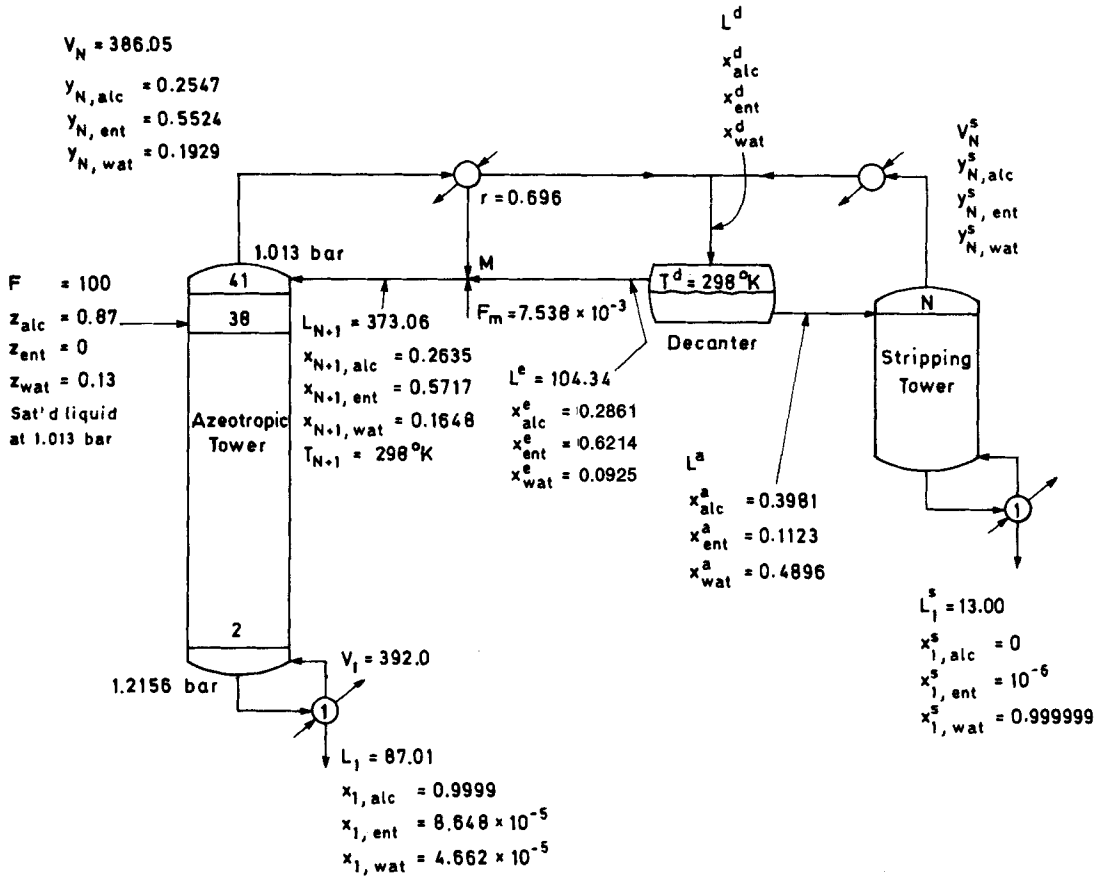

Figure 5. Feasible operating conditions with high recovery of alcohol in the azeotropic tower.

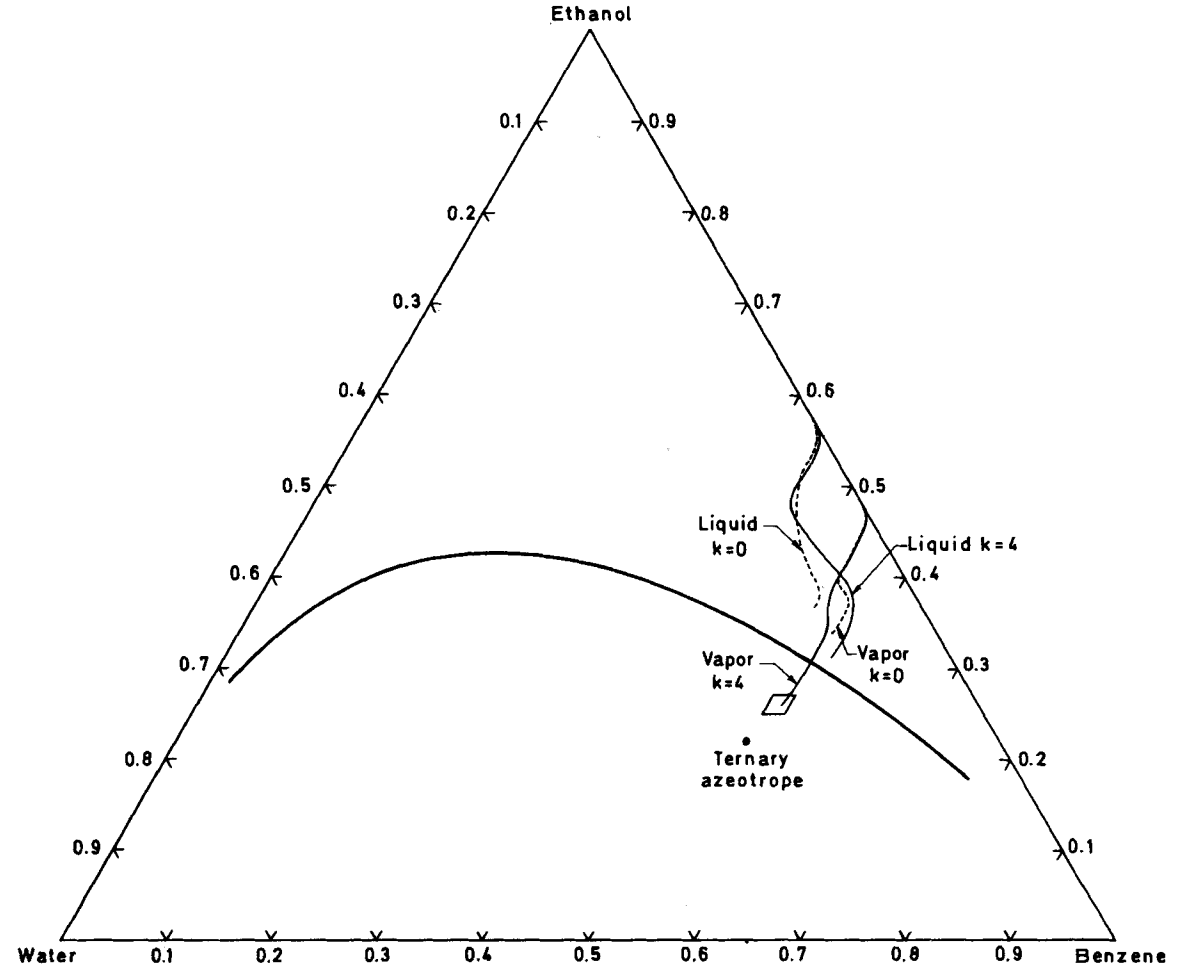

Figure 6. Profiles of vapor and liquid mole fractions initially ($k = 0$) and after the last iteration ($k = 4$) of Powell's method for 41 tray tower.

where the bounds on x^d_{alc} and x^d_{ent} keep $\underline{x}^d$ within the binodal curve. We use Powell's method to solve P4 with numerical derivatives for ∇f and analytical derivatives for the Jacobian matrix, $\underline{\underline{K}}$.

STRIPPING TOWER

Given the solution to P3, L^s_1 and $\underline{x}^s_1$ are computed by overall mass balance and it remains to determine L_a, V^s_N, and $\underline{y}^s_N$, and to design a stripping tower.

Material balances for the species in the decanter are:

$$(1-r)V_N y_{N,j} + V^s_N y^s_{N,j} = L^e x^e_j + L^a x^a_j \quad j = 1, 2, 3 \quad (20)$$

and for the stripper:

$$L^a x^a_j = V^s_N y^s_{N,j} + L^s_1 x^s_{1,j} \quad j = 1, 2, 3 \quad (21)$$

and, for the unknown mole fractions,

$$\sum_{j=1}^{3} y^s_{N,j} = 1 \quad (22)$$

These seven equations have five unknowns, but only four equations are independent since Eq. 20 minus Eq. 21 gives the overall mass balances

$$(1-r)V_N y_{N,j} = L^e x^e_j + L^s_1 x_{1,j} \quad j = 1, 2, 3 \quad (23)$$

which have been satisfied. Hence, there are four independent equations, five unknowns, and one design variable; for example, L^a.

Furthermore, following the logic of Van Dongen and Doherty (1979), all values of L^a place $\underline{y}^s_N$ and $\underline{x}^s_1$ in the same region of the residue curves for simple distillation. Hence, it should be possible to select N, the location of the feed tray, and the reflux ratio to make the separation.

RESULTS

Calculations were performed for a 41 tray tower (including the reboiler) to dehydrate a stream containing 87 mol/s of ethanol and 13 mol/s of water. This feed is a saturated liquid introduced on Tray 38 and the entrainer is benzene.

We solved P3 with the bounds in Eq. 1 and $V^L_1 = 360$ mol/s, $R^L_{alc} = 0.99$, $R^U_{alc} = 1.0$; $x^U_{1,ent} = x^U_{1,wat} = 10^{-4}$; $x^s_{1,ent} = 10^{-6}$; and $T_{N+1} = 298$ K [temperature at which Prausnitz and coworkers (1980) fit the LLE data of Bancroft and Hubard (1942)]. Powell's algorithm was initialized with the guessed values, $V^*_1 = 415.1$ mol/s, $R^*_{alc} = 0.99$, $x^*_{1,ent} = 0.8762 \times 10^{-4}$, $x^*_{1,wat} = 0.4594 \times 10^{-4}$, and the convergence criterion (less than 0.01% deviation of f from a projection of the minimum by Powell's algorithm) was satisfied in four iterations, with $V_1 = 392.0$ mol/s, $R_{alc} = 1.0$, $x_{1,ent} = 0.8648 \times 10^{-4}$ and $x_{1,wat} = 0.4662 \times 10^{-4}$. These results are shown in Figure 5. The profiles of vapor and liquid mole fractions initially and after the last iteration are illustrated in Figure 6, which shows that Powell's algorithm has moved $\underline{y}_N$ into the feasible window. Figure 7 illustrates more clearly the steep fronts in composition and temperature.

TABLE 2. FLOW RATES FOR DEHYDRATION OF ETHANOL WITH BENZENE

Tray	V_i	L_i
41	386.0	424.3
40	437.2	425.6
39	438.6	424.2
38	437.2	521.6 (Feed Tray)
...	...	...
...	...	...
...	...	...
11	438.7	524.7
10	437.7	521.4
9	434.4	511.8
8	424.8	495.4
7	408.4	483.2
6	396.2	479.4
5	392.4	478.8
...	...	...
...	...	...
...	...	...
2	391.8	479.0
1	392.0	87.01

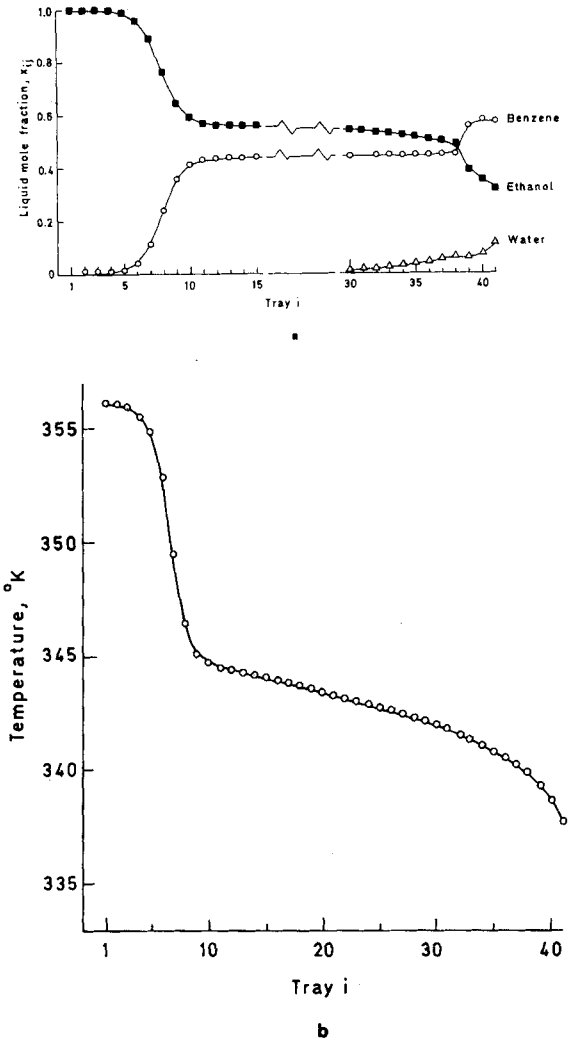

Figure 7. Concentration and temperature profiles for dehydration of ethanol with benzene. $V_1 = 392.0$ mol/s, $R_{alc} = 1.0$, $x_{1,ent} = 0.8648 \times 10^{-4}$, $x_{1,wat} = 0.4662 \times 10^{-4}$, $T_{N+1} = 298$ K, and $x^s_{1,ent} = 10^{-6}$.

The vapor and liquid flow rates in Table 2 show significant changes through the concentration and temperature fronts in the stripping section. From Trays 5–11, the vapor flow rate increases from 392.4 to 438.7 mol/s, an increase of 11.8%, and the liquid flow rate increases from 478.8 to 524.7 mol/s, an increase of 9.6%. Elsewhere, the changes are negligible, with the exception of the overhead vapor condensed by the subcooled reflux on the top tray ($T_{N+1} = 298$ K).

To further demonstrate the importance of the energy balance, P3 was solved assuming constant molal overflow. The mole fraction profiles were in close agreement with Figure 7, but the vapor boil-up rate was 423.1 mol/s (compared with 392.0 mol/s) and the liquid flow rate in the stripping section was 510.1 mol/s.

Finally, Table 3 presents the iteration history for Powell's algorithm in the solution of P3 with the energy balance. Initially, h_2, h_6, and h_7 are active and constraint h_5 is violated. After iteration 1, the overhead vapor can be condensed into two liquid phases and h_6 and h_7 become inactive. For this, and the next two iterations, h_2 remains active and h_5 is violated. α is unity for two iterations and reduced to 0.1 for the last two iterations. The convergence

TABLE 3. ITERATION HISTORY OF POWELL'S METHOD FOR SOLUTION OF P3

	Guessed Values	$k = 1$	$k = 2$	$k = 3$	$k = 4$
α		1.0	1.0	0.1	0.1
f		0.867×10^{-3}	0.718×10^{-3}	0.645×10^{-3}	0.472×10^{-3}
V_1	415.1	402.4	398.3	395.6	392.0
R_{alc}	0.99	1.00	1.00	1.00	1.00
$x_{1,ent}$	0.8762×10^{-4}	0.8647×10^{-4}	0.8647×10^{-4}	0.8647×10^{-4}	8.648×10^{-4}
$x_{1,wat}$	0.4591×10^{-4}	0.4601×10^{-4}	0.4594×10^{-4}	0.4624×10^{-4}	0.4662×10^{-4}
Constraints Violated	h_5	h_5	h_5	h_5	None
Constraints Active	h_2,h_6,h_7	h_2	h_2	h_2	h_2
$y_{N,alc}$	0.3430	0.2454	0.2479	0.2494	0.2547
$y_{N,ent}$	0.5615	0.5543	0.5534	0.5528	0.5524
$y_{N,wat}$	0.0955	0.2003	0.1987	0.1978	0.1929

criteria are satisfied after iteration 4, with no constraints violated.

In addition, calculations were performed for a 27 tray tower (including the reboiler) to dehydrate a stream containing 89 mol/s of ethanol and 11 mol/s of water. This saturated liquid feed at 1.013 bar is introduced on Tray 22 and the entrainer is benzene. The tower was designed by Robinson and Gilliland (1950) and simulated by Magnussen and coworkers (1979). The latter report three steady states for the same specifications ($L^e + F_m = 45.32$ mol/s and containing 9.9 mol/s ethanol, 33.62 mol/s benzene, and 1.8 mol/s water), but they assume constant molal overflow and compute $V_1 = 408.3$ mol/s for the three steady states. With the energy balance, V_1 varies and, hence, their results differ somewhat from the actual physical process.

The Magnussen results show three distinct regimes of operation that we observed as well (Prokopakis et al., 1981). These have the following characteristics:

1. *Regime I.* Water is removed gradually near the top of the stripping section. Entrainer and alcohol maintain nearly constant mole fractions until the entrainer is eliminated in a steep front on the bottom few trays.

2. *Regime II.* The entrainer is removed near the top of the stripping section and the water is gradually eliminated throughout the stripping section.

3. *Regime III.* Alcohol is present in high concentration throughout the stripping section, often nearly pure. Although in the Magnussen results, it is diluted by about 7.5 mol % water throughout the entire tower.

An objective in this work was to solve P3 with bounds on the design variables just above and below those computed by Mag-

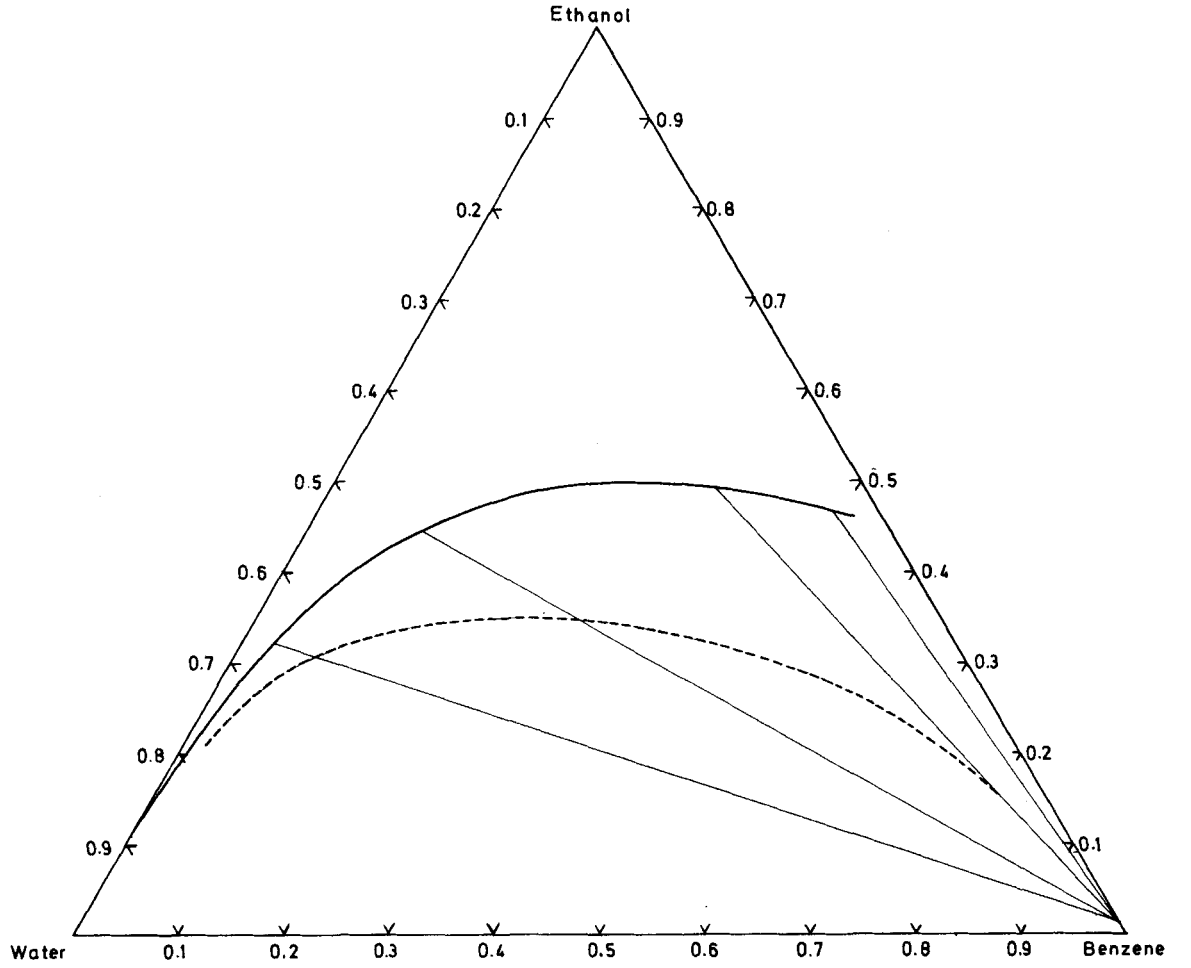

Figure 8. Binodal curve computed using the UNIQUAC equation with interaction coefficients by Gmehling and Onken (1977) who fit the vapor-liquid equilibrium data of Norman (1945) (Solid line with tie-lines). See Table 1 for parameters. The dashed line shows the experimental binodal curve at 337.5 K of Norman (1945).

nussen and coworkers, in the hope that, with small adjustments in the design variables, $\underline{y}_N$ could be located in the feasible window with constraints h_6 and h_7 satisfied for each of their three steady-state solutions. Unfortunately, however, Magnussen and coworkers used the UNIQUAC equation with the parameters of Gmehling and Onken (1977), who fit vapor-liquid equilibrium data (Norman, 1945) without liquid-liquid equilibrium data. Consequently, their estimates of the compositions of two liquids in equilibrium are poor, as illustrated in Figure 8; the region of immiscibility is too broad and the entrainer phases contain less than 3 mol % of alcohol. With this data, the design variables can be easily adjusted to locate $\underline{y}_N$ in the feasible window, but since the aqueous phase leaving the decanter contains the bulk of the alcohol, constraints h_6 and h_7 cannot be satisfied with a high recovery of alcohol in the azeotropic tower; that is with $R^L_{alc} \geq 0.85$, as computed by Magnussen and coworkers.

Consequently, we had to abandon the Gmehling and Onken parameters in favor of those by Prausnitz and coworkers, and with this, our objective to confirm the existence of their steady-state multiplicity. Instead, we sought to locate design variables that correspond to operation in each of the three regimes.

Regime I

To obtain Regime I, we solved P3 with the bounds in Eq. 1 and $V^L_1 = 250$ mol/s; $R^L_{alc} = 0.9$, $R^U_{alc} = 1.0$, $x^U_{1,ent} = x^U_{1,wat} = 5 \times 10^{-4}$; $T_{N+1} = 298$ K, and $x^s_{1,ent} = 10^{-6}$. Powell's algorithm was initialized with the guessed values, $V^*_1 = 425$ mol/s, $R^*_{alc} = 0.96$, $x^*_{1,ent} = 2.6 \times 10^{-4}$, $x^*_{1,wat} = 3.0 \times 10^{-4}$, and the convergence criteria were satisfied in four iterations, with $V_1 = 443.4$ mol/s; $R_{alc} = 0.909$, $x_{1,ent} = 2.5 \times 10^{-4}$; $x_{1,wat} = 2.45 \times 10^{-4}$ and

$$L_1 = 81.0 \text{ mol/s}$$

$$V_N = 442.8 \text{ mol/s}, \underline{y}_N = [0.2586\ 0.5529\ 0.1885]^T$$

$$L_{N+1} = 423.7 \text{ mol/s}, \underline{x}_{N+1} = [0.2512\ 0.5777\ 0.1711]^T$$

$$F_m = 0.0199 \text{ mol/s}$$

$$L^e = 64.75 \text{ mol/s}, \underline{x}^e = [0.2107\ 0.7144\ 0.0749]^T$$

$$\underline{x}^a = [0.3480\ 0.0635\ 0.5885]^T$$

$$r = 0.8103, \mathcal{R} = 4.27$$

where $\mathcal{R} = r/(1-r)$ is the reflux ratio. The profiles of liquid mole fractions are in Figure 9 and the flow rates increase by approximately 12% through the concentration and temperature fronts in the stripping section.

Figure 9 shows the close agreement with the profiles of Mag-

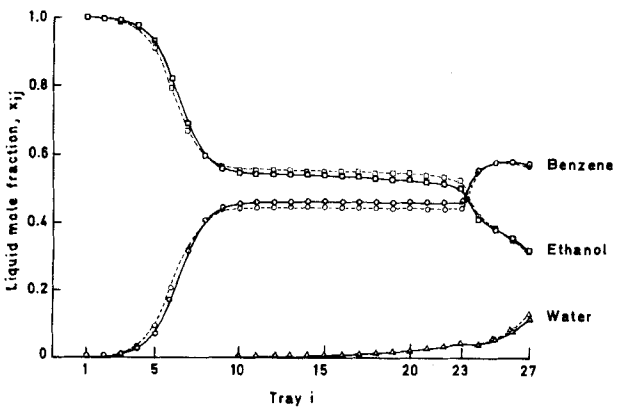

Figure 9. Regime I concentration profiles. Solid lines were computed by solution of the MESH equations and P3 ($V_1 = 443.4$ mol/s, $R_{alc} = 0.909$, $x_{1,ent} = 2.5 \times 10^{-4}$, $x_{1,wat} = 2.45 \times 10^{-4}$, $\mathcal{R} = 4.27$) with interaction coefficients for the UNIQUAC equation by Prausnitz and coworkers (1980); see Table 1. Dashed lines were computed by solution of the MES equations (Magnussen et al., 1979. $V_1 = 408.3$ mol/s, $R_{alc} = 0.923$, $x_{1,ent} = 2.6 \times 10^{-4}$, $x_{1,wat} = 3.0 \times 10^{-4}$, $\mathcal{R} = 5.47$) with interaction coefficients by Gmehling and Onken (1977).

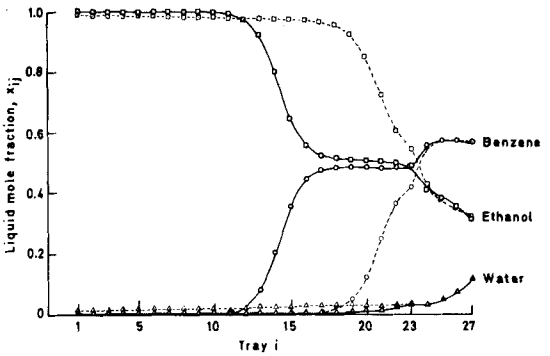

Figure 10. Regime II concentration profiles. Solid lines were computed by solution of P3 ($V_1 = 598.1$ mol/s, $R_{alc} = 0.947$, $x_{1,ent} = 1.55 \times 10^{-8}$, $x_{1,wat} = 1.76 \times 10^{-3}$, $\mathcal{R} = 4.87$). Dashed lines were computed by Magnussen and coworkers ($V_1 = 408.3$ mol/s, $R_{alc} = 0.921$, $x_{1,ent} = 2.6 \times 10^{-8}$, $x_{1,wat} = 3.3 \times 10^{-3}$, $\mathcal{R} = 5.47$).

nussen and coworkers, obtained with $V_1 = 408.3$ mol/s, $R_{alc} = 0.923$, $x_{1,ent} = 2.6 \times 10^{-4}$, $x_{1,wat} = 3.0 \times 10^{-4}$, and $\mathcal{R} = 5.47$.

Regime II

To obtain Regime II, we solved P3 with the bounds in Eq. 1 and $V^L_1 = 250$ mol/s, $R^L_{alc} = 0.9$, $R^U_{alc} = 1.0$, $x^U_{1,ent} = 5 \times 10^{-8}$, $x^U_{1,wat} = 5 \times 10^{-3}$, $T_{N+1} = 298$ K, and $x^s_{1,ent} = 10^{-6}$. Powell's algorithm was initialized with the guessed values, $V^*_1 = 407.5$ mol/s, $R^*_{alc} = 0.96$, $x^*_{1,ent} = 2.6 \times 10^{-8}$, $x^*_{1,wat} = 3.3 \times 10^{-3}$ and the convergence criteria were satisfied in six iterations, with $V_1 = 598.1$ mol/s, $R_{alc} = 0.947$, $x_{1,ent} = 1.55 \times 10^{-8}$, $x_{1,wat} = 1.76 \times 10^{-3}$ and

$$L_1 = 84.4 \text{ mol/s}$$

$$V_N = 595.8 \text{ mol/s}, \underline{y}_N = [0.2599\ 0.5526\ 0.1875]^T$$

$$L_{N+1} = 580.2 \text{ mol/s}, \underline{x}_{N+1} = [0.2587\ 0.5675\ 0.1738]^T$$

$$F_m = 1.69 \times 10^{-5} \text{ mol/s}$$

$$L^e = 85.6 \text{ mol/s}, \underline{x}^e = [0.2526\ 0.6519\ 0.0955]^T$$

$$\underline{x}^a = [0.3834\ 0.0870\ 0.5296]^T$$

$$r = 0.8296, \mathcal{R} = 4.87$$

The profiles of liquid mole fractions are in Figure 10. The steep composition fronts differ in position from those of Magnussen and coworkers, obtained with $V_1 = 408.3$ mol/s, $R_{alc} = 0.921$, $x_{1,ent} = 2.6 \times 10^{-8}$, $x_{1,wat} = 3.3 \times 10^{-3}$ and $\mathcal{R} = 5.47$. Probably, this disparity is due to the difference in interaction coefficients for the UNIQUAC equation.

Regime III

To obtain Regime III, we attempted to solve P3 with the bounds in Eq. 1 and $V^L_1 = 250$ mol/s, $R^L_{alc} = 0.85$, $R^U_{alc} = 1.0$, $x^U_{1,ent} = 10^{-4}$, $x^U_{1,wat} = 0.08$, $T_{N+1} = 298$ K, and $x^s_{1,ent} = 10^{-6}$. Powell's algorithm was initialized with the guessed values, $V^*_1 = 407.5$ mol/s, $R^*_{alc} = 0.93$, $x^*_{1,ent} = 10^{-14}$, and $x^*_{1,wat} = 0.08$. After three iterations, $\underline{y}_N$ was located in the feasible window, but constraints $h_2 - h_4$ were active and h_6 and h_7 were violated, with $V_1 = 427.7$ mol/s, $R_{alc} = 0.85$, $x_{1,ent} = 10^{-14}$, $x_{1,wat} = 0.08$, $r = 1.17$, and $L^e = -91.03$ mol/s. No improvement was obtained in subsequent iterations. After iteration 3,

$$L_1 = 82.2 \text{ mol/s}$$

$$V_N = 428.2 \text{ mol/s}, \underline{y}_N = [0.2662\ 0.5533\ 0.1805]^T$$

$$L_{N+1} = 410.4 \text{ mol/s}, \underline{x}_{N+1} = [0.2451\ 0.5774\ 0.1775]^T$$

$$F_m = 1.7777 \times 10^{-5} \text{ mol/s}$$

and Figure 11 shows the profiles of liquid mole fractions. These

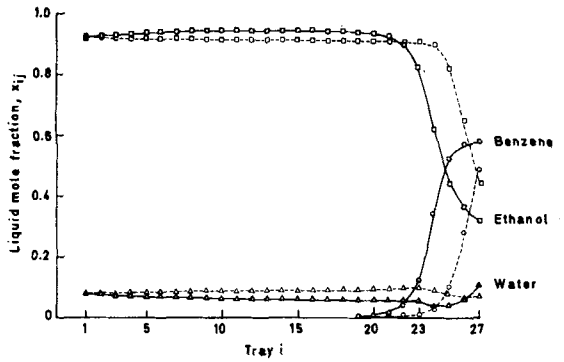

Figure 11. Regime III concentration profiles. Solid lines were computed by solution of P3 ($V_1 = 427.7$ mol/s, $R_{alc} = 0.85$, $x_{1,ent} = 10^{-14}$, $x_{1,wat} = 0.08$, $\mathcal{R} = -6.88$). Dashed lines were computed by Magnussen and coworkers ($V_1 = 408.3$ mols/s, $R_{alc} = 0.854$, $x_{1,ent} = 4.0 \times 10^{-15}$, $x_{1,wat} = 0.075$, $\mathcal{R} = 5.47$).

are comparable to those of Magnussen and coworkers, obtained with $V_1 = 408.3$ mol/s, $R_{alc} = 0.854$, $x_{1,ent} = 4.0 \times 10^{-15}$, $x_{1,wat} = 0.075$ and $\mathcal{R} = 5.47$. However, in the latter results $\underline{y}_N$ ($[0.3621\ 0.5328\ 0.1051]^T$) lies outside the binodal curve the vapor overhead stream cannot be condensed into two liquid phases. Hence, feasible operating conditions can be achieved with a vapor overhead stream from the stripping tower below the decanter tie-line and, consequently, with low recovery of alcohol in the azeotropic tower.

In an attempt to locate Regime III with $R^L_{alc} \geq 0.85$, we lowered $x^U_{1,ent}$ and $x^U_{1,wat}$, and obtained impractically high V_1. Hence, we conclude that Regime III cannot be obtained with high recovery of alcohol in this 27 tray tower.

APPENDIX

The algorithm in Figure 12 solves the MESH equations on Tray i for V_i, L_{i+1}, $\underline{x}_{i+1}$, and T_{i+1} (and y_{i+1}), given $\underline{x}_i$, y_i, and T_i from solution of the MESH equations on the tray below. For the reboiler (Tray 1), V_1 is specified and the energy balance is solved for Q_1; hence, the inner iteration loop is unnecessary. For Tray N, T_{N+1} is specified and Step 4 is eliminated.

ACKNOWLEDGMENT

The assistance of C. W. White, III, in the usage of Powell's algorithm is appreciated. Computing time was provided by the School of Engineering and Applied Science at the University of Pennsylvania.

Given $\underline{x}_i$, $\underline{y}_i$, T_i, from the solution of the MESH eqns. on the tray below:

1. Guess $V_i^* = V_{i-1}$
2. Compute L_{i+1}

$$L_{i+1} = V_i + L_1 \quad i < i_{feed}$$

$$L_{i+1} = V_i + L_1 - F \quad i \geq i_{feed}$$

3. Compute $\underline{x}_{i+1}$

$$\underline{x}_{i+1} = (\underline{y}_i V_i + \underline{x}_1 L_1)/L_{i+1} \quad i < i_{feed}$$

$$\underline{x}_{i+1} = (\underline{y}_i V_i + \underline{x}_1 L_1 - \underline{z} F)/L_{i+1} \quad i \geq i_{feed}$$

4. Find bubble point T_{i+1}, $\underline{y}_{i+1}$
5. Compute V_i

$$V_i = (L_{i+1} h^L_{i+1} + Q_1 - L_1 h^L_1)/h^V_i \quad i < i_{feed}$$

$$V_i = (L_{i+1} h^L_{i+1} + Q_1 - L_1 h^L_1 + F h^F)/h^V_i \quad i \geq i_{feed}$$

6. Is

$$\left|\frac{V_i - V_i^*}{V_i}\right| \leq \epsilon ?$$

No. $V_i^* = V_i$

Yes. $i = i + 1$

Figure 12. Algorithm for solution of the MESH equations on Tray i.

NOTATION

$\underline{d}$ = vector of changes in design variables computed by quadratic programming algorithm
f = objective function
$\hat{f}$ = residual of Eq. 19
F = flow rate of feed
$\underline{g}$ = vector of equality constraints
$\underline{h}$ = vector of inequality constraints
$\underline{\hat{h}}$ = vector of inequality constraints, P4
$\underline{\underline{J}}$ = Jacobian matrix of equality constraints
$\underline{\underline{K}}$ = Jacobian matrix of inequality constraints
L = liquid flow rate; Lagrangian function
m = number of inequality constraints
P = pressure
r = fraction of condensate that bypasses the decanter
R = fractional recovery in bottoms product
$\mathcal{R}$ = reflux ratio
T = temperature
V = vapor flow rate
V_1 = boil-up rate
$\mathcal{V}_1$ = dimensionless boil-up rate, Eq. 8
x = liquid mole fraction, design variable
$\underline{x}$ = vector of liquid mole fractions; vector of design variables see Eq. 8
y = vapor mole fraction
$\underline{y}$ = vector of vapor mole fractions
z = mole fraction of feed
$\underline{z}$ = vector of feed mole fractions, vector of slack variables

Greek Symbols

α = parameter in unidirectional search, Eq. 5
$\underline{\beta}$ = vector of coefficients in Eq. 19
$\underline{\gamma}$ = vector of liquid phase activity coefficients
$\underline{\Lambda}$ = vector of Lagrange multipliers
λ_i^* = see Eq. 7
$\underline{\pi}$ = vector of Kuhn-Tucker multipliers
π_i^* = see Eq. 6
ϕ = objective function in Han unidirectional search

Subscripts

alc = alcohol
ent = entrainer
i = tray number (reboiler is Tray 1), counter
m = entrainer make-up
N = number of trays (including the reboiler), top tray
wat = water

Superscripts

a = aqueous phase from decanter
d = feed to the decanter
e = entrainer phase from decanter
k = iteration counter in Powell's method
L = lower bound
s = stripping tower
T = transpose
U = upper bound
$*$ = solution of P1

LITERATURE CITED

Bancroft, W. D., and S. S. Hubard, "A New Method for Determining Dineric Distribution," *J. Amer. Chem. Soc.*, **64**, 347 (1942).

Benedict, M., and L. C. Rubin, "Extractive and Azeotropic Distillation," *Trans. AIChE*, **41**, 353 (1945).

Berna, T. J., M. H. Locke, and A. W. Westerberg, "A New Approach to Optimization of Chemical Processes," *AIChE J.*, **26**, 1 (1980).
Biegler, L. T., and R. R. Hughes, "Approximation Programming of Chemical Processes with Q/LAP," *Chem. Eng. Prog.*, (April, 1981).
Black, C., R. A. Golding, and D. E. Ditsler, "Azeotropic Distillation Results from Automatic Computer Calculations," *Extractive and Azeotropic Distillation*, Advances in Chemistry Series 115, ACS (1972).
Boston, J. F., "Algorithms for Distillation Calculations with Bounded-Variable Design Constraints and Equality- or Inequality-Constrained Optimization," Energy Laboratory, M.I.T., Cambridge, MA (1978).
Gmehling, J., and U. Onken, *Vapor-Liquid Equilibrium Data Collection*, DECHEMA, Chemistry Data Series, I, Part 1, Verlag & Druckerei Friedrick Bischoff, Frankfurt (1977).
Jirapongphan, S., *Simultaneous Modular Convergence Concept in Process Flowsheet Optimization*, D.Sc Dissertation, M.I.T. (1980).
Jirapongphan, S., J. F. Boston, H. I. Britt, and L. B. Evans, "A Nonlinear Simultaneous Modular Algorithm for Process Flowsheet Optimization," Dept. of Chem. Eng. and Energy Lab., M.I.T., Cambridge, MA (1980).
Magnussen, T., M. L. Michelsen, and A. Fredenslund, "Azeotropic Distillation Using UNIFAC," *Inst. Chem. Eng. Symp. Ser. No. 56*, Third Int'l Symp. on Distillation, ICE, Rugby, Warwickshire, England (1979).
Napthali, L. M., and D. P. Sandholm, "Multicomponent Separation Calculations by Linearization," *AIChE J.*, **17**, 1 (1971).
Norman, W. S., "The Dehydration of Ethanol by Azeotropic Distillation, Vapour-Liquid Equilibrium Data for the System Ethanol-Benzene-Water," *Trans. Inst. Chem. Eng.*, **23**, 66 (1945).
Powell, M. J. D., "A Fast Algorithm for Nonlinearly Constrained Optimization Calculations," presented at 1977 Dundee Conference on Numerical Analysis (1977).
Prausnitz, J. M., T. F. Anderson, E. A. Grens, C. A. Eckert, R. Hsieh, and J. P. O'Connell, *Computer Calculations for Multicomponent Vapor-Liquid and Liquid-Liquid Equilibria*, Prentice-Hall (1980).
Prokopakis, G. J., and W. D. Seider, "Dynamic Simulation of Distillation Towers," presented at the 73rd Annual Meeting of AIChE, Chicago (1980).
Prokopakis, G. J., B. A. Ross, and W. D. Seider, "Azeotropic Distillation Towers with Two Liquid Phases," *Foundations of Computer-aided Chemical Process Design*, eds., R. S. H. Mah and W. D. Seider, AIChE (1981).
Reid, R. C., J. M. Prausnitz, and T. K. Sherwood, *Properties of Gases and Liquids*, Third Edition, McGraw-Hill (1977).
Robinson, C. S., and E. R. Gilliland, *Elements of Fractional Distillation*, McGraw-Hill, p. 312 (1950).
Ross, B. A., and W. D. Seider, "Simulation of Three-Phase Distillation Towers," *Comp. and Chem. Eng.*, **5**, 1 (1981).
Van Dongen, D. B., and M. F. Doherty, "Restrictions on the Behavior of Multicomponent Azeotropic Distillation Processes," Paper No. 66C, 72nd Annual Meeting of AIChE, San Francisco, CA (1979).

Manuscript received August 4, 1981; revision received January 26, and accepted February 22, 1982.

Absorption of Sulfur Dioxide into Aqueous Double Slurries Containing Limestone and Magnesium Hydroxide

The absorption of dilute SO_2 into aqueous double slurries containing $CaCO_3$ and $Mg(OH)_2$ was carried out using a stirred tank with a plane gas-liquid interface. The absorption rate increased and finally reached that under the completely gas-film controlled conditions as the absorption process proceeded. The desulfurization process using the double slurry was formulated by a two-reaction-plane model in which there are no particles suspended in-between the interface and the primary reaction plane. It was suggested from comparison of the experimental absorption rates with the theoretical predictions that 40 to 60% of the absorbed sulfur dioxide may be present as an effective magnesium sulfite ion pair.

E. SADA, H. KUMAZAWA
and
H. NISHIMURA

Department of Chemical Engineering
Kyoto University
Kyoto, Japan

SCOPE

The elementary processes involved in chemical absorption into a slurry are: (i) diffusion of solute gas in the gas film, (ii) diffusion in the liquid film, (iii) chemical reaction, and (iv) dissolution of solids (one of the reactants). Elementary process (ii) combined with (iii) is called chemical absorption or gas absorption accompanied by chemical reaction. The chemical absorption and the solid dissolution are transfer processes in parallel or in series, depending upon whether the suspended particle size is much smaller than or is comparable to the thickness of the liquid film. When this transfer process is assumed to be serial, it can be analyzed in terms of conventional chemical absorption theories. When the process is assumed to be in parallel, on the other hand, the absorption rate is influenced by coexistence of solid dissolution. That is, the dissolution of solids which can suspend in the liquid film enhances the absorption rate; the rate of solid dissolution is enhanced by the reaction between the dissolved gas and the dissolved solid in the liquid film.

The reaction in flue gas desulfurization using a slurry is regarded as being both consecutive and parallel. Evaluation of the desulfurization rate or the efficiency is further complicated by the coexistence of the solid dissolution. For example, the chemical reactions accompanying SO_2 absorption into $Mg(OH)_2$ slurry are considered to be

$$SO_2 + SO_3^{2-} + H_2O \rightarrow 2HSO_3^- \qquad (i)$$

and

0001-1541-83-6426-0060-$2.00.